Multi-physical Modeling and Multi-scale Computation of Nano-Optical Responses

Gang Bao, Guanghui Hu, Di Liu, and Songting Luo

Abstract. Our recent study of multi-physical modeling and multi-scale computation of nano-optical responses is presented in this paper. The semi-classical theory treats the evolution of the electromagnetic (EM) field and the motion of the charged particles concurently by coupling Maxwell equations with Quantum Mechanics. A new efficient computational framework is proposed in [**1, 2**] by integrating the Time Dependent Current Density Functional Theory (TD-CDFT), which leads to the coupled Maxwell-Kohn-Sham equations determining the EM field as well as the current and electron densities simultaneously. In the regime of linear responses, a self-consistent multi-scale method is proposed to deal with the well separated space scales. Related recent research on developing adaptive Finite Element Methods for the Kohn-Sham equation [**3, 4**] is also discussed.

1. Multi-Physical Modeling and Nano-Optics

The study of optical responses of nano structures has generated a lot of interest in the development of modern physics. When the optical device is of nano scale, the macroscopic theory for the electromagnetic (EM) field based on constitutive relations can not faithfully capture the microscopic and nonlocal characteristics of the light-matter interaction. In this case, it is necessary to consider the quantum mechanical description of the current and charge densities. Quantum Electrodynamics (QED) [**5**] is able to give a complete description of the interactions between photons and electrons. However, the high computational expense prohibits QED from applications. The semi-classical theories [**6, 7, 8**] combine the classical treatment of the EM field and the first principle approach for the charged particles. Different from QED, in a semi-classical theory, the EM field is not quantized and its time evolution is described classically by the Maxwell equations. In the meantime, the motion of charged particles is determined quantum mechanically by Schrödinger equations. To avoid solving the high dimensional many body Schrödinger equation

1991 *Mathematics Subject Classification.* 78A45, 81-08, 81V55.

Key words and phrases. Optical response, Nanostructures, Multiscale methods, Adaptive methods, Density Functional Theory.

The research is supported in part by the NSF FRG DMS-0968360. G. Bao's research was also supported in part by the NSF grants DMS-0908325, CCF-0830161, EAR-0724527, DMS-1211292, the ONR grant N00014-12-1-0319, a Key Project of the Major Research Plan of NSFC (No. 91130004), and a special research grant from Zhejiang University. D. Liu's research was also supported partially by NSF Career Award DMS-0845061.

involved in the semi-classical theory, in [**1, 2**], we adopted the Time Dependent Current Density Functional Theory (TD-CDFT) [**9, 10**] to further simplify the model and its computation.

1.1. The semi-classical theory for nano-optics. The semi-classical theory for nano-optical responses combines classical treatment of the EM field and quantum mechanical description of the charged particles. The evolution of the EM field can be determined by Maxwell equations. In terms of the vector potential $\mathbf{A}$ and scalar potential ϕ, under the Coulomb gauge $\nabla \cdot \mathbf{A} = 0$, the Maxwell equations have the form:

$$\begin{aligned} \frac{1}{c^2}\frac{\partial^2 \mathbf{A}}{\partial t^2} - \nabla^2 \mathbf{A} + \frac{1}{c}\frac{\partial(\nabla\phi)}{\partial t} &= \frac{4\pi}{c}\mathbf{j}, \\ -\nabla^2\phi &= 4\pi\rho, \end{aligned} \tag{1.1}$$

where c is the speed of light in vacuum, and $\mathbf{j}$ and ρ are the current density and charge density related by the continuity equation:

$$\nabla \cdot \mathbf{j} + \frac{\partial \rho}{\partial t} = 0. \tag{1.2}$$

The electric and magnetic fields, $\mathbf{E}$ and $\mathbf{B}$, can be evaluated by

$$\mathbf{E} = -\nabla\phi - \frac{1}{c}\frac{\partial \mathbf{A}}{\partial t}, \qquad \mathbf{B} = \nabla \times \mathbf{A}. \tag{1.3}$$

Notice that in the Maxwell equations, ρ and $\mathbf{j}$ serve as input to compute the EM field. In a classical macroscopic model, they would be determined by the so called constitutive relations as local functions in terms of $\mathbf{E}$ and $\mathbf{B}$. When the size of the sample is of nano scale such that the spatial structure of the resonant states is comparable to or even larger than the wavelength of the light, a microscopic nonlocal treatment must be considered.

Quantum mechanically, the motion of the charged particles is governed by the Schrödinger equation. For a system consisting of N electrons moving under the influence of a given transverse EM field represented by $\mathbf{A}$, the general nonrelativistic Hamiltonian takes the form [**5, 8**]:

$$H_M = \frac{1}{2}\sum_l \left[\mathbf{p}_l + \frac{1}{c}\mathbf{A}(\mathbf{r}_l)\right]^2 + \sum_l v(\mathbf{r}_l) + U, \tag{1.4}$$

where $\mathbf{r}_l$ and $\mathbf{p}_l$ are the coordinate and conjugate momentum of the lth electron, $v(\mathbf{r})$ is the single particle external potential due to the nuclei, and $U = \frac{1}{2}\sum_{l\neq l'} \frac{1}{|\mathbf{r}_l - \mathbf{r}_{l'}|}$ is the mutual Coulomb interaction among electrons. For simplicity, we will assume the Born-Oppenheimer approximation to separate the electronic motion and the nuclear motion for the molecular structures under consideration.

After the incident light is applied, the system will evolve according to the time dependent Schrödinger equation

$$i\frac{\partial \psi(\mathbf{r}_1, ..., \mathbf{r}_N, t)}{\partial t} = H_M \psi(\mathbf{r}_1, ..., \mathbf{r}_N, t). \tag{1.5}$$

The current density $\mathbf{j}(\mathbf{r}, t)$ and electron density $\rho(\mathbf{r}, t)$ can be computed through solutions of (1.5) using

$$\mathbf{j}(\mathbf{r}, t) = < \psi | \hat{\mathbf{j}} | \psi > \quad \text{and} \quad \rho(\mathbf{r}, t) = < \psi | \hat{\rho} | \psi >, \tag{1.6}$$

with the current density operator $\hat{\mathbf{j}}$ and electron density operator $\hat{\rho}$ being given respectively by

$$\begin{aligned} \hat{\mathbf{j}} &= -\frac{1}{2}\sum_l \Big[\mathbf{p}_l\delta(\mathbf{r}-\mathbf{r}_l) + \delta(\mathbf{r}-\mathbf{r}_l)\mathbf{p}_l\Big] - \frac{1}{c}\sum_l \mathbf{A}(\mathbf{r}_l,t), \\ \hat{\rho} &= -\sum_l \delta(\mathbf{r}-\mathbf{r}_l). \end{aligned} \tag{1.7}$$

Notice that in Schrödinger equation (1.5), $\mathbf{A}$ acts as parameters for computing the wavefunction ψ, which will give all physical observables including current and electron densities.

In the semi-classical model, the system is completely described by $(\mathbf{A},\phi)$ and ψ, which affect each other through the coupled Maxwell equations (1.1) and Schrödinger equation (1.5). Therefore they must be determined self-consistently so that equations (1.1) and (1.5) are solved concurrently, which will give rise to the evolution of the EM field and the motion of electrons simultaneously.

1.2. Time dependent current density functional theory. Although the semi-classical theory greatly simplifies the modeling of light-matter interactions at the nano scale, it still poses a significant numerical challenge to solve the high dimensional many body Schrödinger equation involved. Notice that solving the Maxwell equations (1.1) only requires the input of much simpler quantities of the current density $\mathbf{j}$ and electron density ρ. One efficient way to obtain numerical approximations of $(\mathbf{j},\rho)$ is the Time Dependent Current Density Functional Theory (TD-CDFT). The advantage of TD-CDFT is that by restricting to the current and electron densities that are functions of only 3D spatial variables, the computational cost can be greatly reduced.

In TD-CDFT, a system of time dependent Kohn-Sham (KS) equations can be derived in the following form:

$$i\frac{\partial\varphi_l(t)}{\partial t} = H_M^{KS}(t)\varphi_l(t), \tag{1.8}$$

with the following Hamiltonian:

$$H_M^{KS}(t) = \frac{1}{2}\Big[\mathbf{p} + \mathbf{A}_{KS}(\mathbf{r},t)\Big]^2 + v_{KS}(\mathbf{r},t). \tag{1.9}$$

The time dependent KS potential in the above Hamiltonian is given by

$$v_{KS}(\mathbf{r},t) = v(\mathbf{r},t) + v_H(\mathbf{r},t) + v_{xc}(\mathbf{r},t), \tag{1.10}$$

with $v_{xc}(\mathbf{r},t)$ representing the time dependent scalar xc-potential, and

$$\mathbf{A}_{KS}(\mathbf{r},t) = \frac{1}{c}\mathbf{A}(\mathbf{r},t) + \mathbf{A}_{xc}(\mathbf{r},t), \tag{1.11}$$

where $\mathbf{A}$ is the vector potential for the external EM field and $\mathbf{A}_{xc}(\mathbf{r},t)$ is the vector xc-potential. The electron density and the current density can be given by

$$\rho(\mathbf{r}) = \sum_l f_l|\varphi_l(\mathbf{r})|^2, \tag{1.12}$$

and

$$\mathbf{j}(\mathbf{r},t) = -\frac{i}{2}\sum_l f_l\Big[\varphi_l^*(\mathbf{r},t)\nabla\varphi_l(\mathbf{r},t) - \varphi_l(\mathbf{r},t)\nabla\varphi_l^*(\mathbf{r},t)\Big] + \sum_l f_l|\varphi_l(\mathbf{r})|^2\mathbf{A}_{KS}(\mathbf{r},t), \tag{1.13}$$

where f_l is the occupation number.

1.3. The Maxwell-KS system. We can incorporate the TD-CDFT into the semi-classical theory by replacing the current density and the electron density (1.6) given by solutions of the Schrödinger equation with those obtained by TD-CDFT using (1.12) and (1.13). Therefore the Maxwell equations (1.1) and the time dependent Kohn-Sham equations (1.8) form a coupled system for the EM field ($\mathbf{A}$, ϕ) and the current and electron densities ($\mathbf{j}$, ρ) as they are functionals of each other, i.e.,

$$\begin{cases} (\mathbf{A},\phi) &= \mathcal{M}\big[\mathbf{j},\rho\big]\ ; \\ (\mathbf{j},\rho) &= \mathcal{T}\big[\mathbf{A},\phi\big]\ , \end{cases} \tag{1.14}$$

which suggests that they must be determined self-consistently. From now on, we will refer the above equations as the Maxwell-Kohn-Sham (Maxwell-KS) equations for nano-optics.

For most applications in nano-optics, the induced EM field is varying on a much larger scale than the induced current and electron densities, when the wavelength of the induced EM field is comparable to or larger than the size of the nano structure. Numerically, the mesh size required for the accuracy and stability of solving the Maxwell equations is much larger than the domain we need to handle with TD-CDFT. As a consequence, the coupled Maxwell-KS system can be very ill-conditioned after direct space discretization.

2. Linear Response Theory

The linear response of the Maxwell-KS system (1.14) will further facilitate the computation. In the regime of linear responses, the self-consistent calculation of $(\mathbf{A},\phi)$ and $(\mathbf{j},\rho)$ results in a simple linear system of equations that will allow us to work in the frequency domain.

2.1. Linearized Maxwell-KS system. Rewriting Maxwell equations in the integral form through Green functions shows that the EM field is actually linear functionals of the electron and current densities. On the other hand, the linear response theory of TD-CDFT [**11, 12, 13**] describes the linear relation between the input of the EM field and the output of the microscopic quantities. Combining both theories will lead to the following linear system for the induced EM field ($\delta\mathbf{A}$,

$\delta\phi$) and the induced electron and current densities ($\delta\mathbf{j}$, $\delta\rho$):

$$
\left\{
\begin{array}{rcl}
\delta\mathbf{A}(\mathbf{r},\omega) &=& -\dfrac{1}{c}\displaystyle\int \mathbf{G}(\mathbf{r}-\mathbf{r}')\delta\mathbf{j}(\mathbf{r}')d\mathbf{r}', \\
\delta\phi(\mathbf{r},\omega) &=& -\displaystyle\int \frac{\delta\rho(\mathbf{r}')}{|\mathbf{r}-\mathbf{r}'|}d\mathbf{r}', \\
\delta\mathbf{j}(\mathbf{r},\omega) &=& \displaystyle\int \Big(\chi_{jj}(\mathbf{r},\mathbf{r}',\omega)-\chi_{jj}(\mathbf{r},\mathbf{r}',0)\Big)\cdot\delta\mathbf{A}_{KS}(\mathbf{r}',\omega)d\mathbf{r}' \\
&& \qquad\qquad + \displaystyle\int \chi_{j\rho}(\mathbf{r},\mathbf{r}',\omega)\delta v_{KS}(\mathbf{r}',\omega)d\mathbf{r}', \\
\delta\rho(\mathbf{r},\omega) &=& \displaystyle\int \chi_{\rho j}(\mathbf{r},\mathbf{r}',\omega)\cdot\delta\mathbf{A}_{KS}(\mathbf{r}',\omega)d\mathbf{r}' \\
&& \qquad\qquad + \displaystyle\int \chi_{\rho\rho}(\mathbf{r},\mathbf{r}',\omega)\delta v_{KS}(\mathbf{r}',\omega)d\mathbf{r}',
\end{array}
\right. \tag{2.1}
$$

where the vector and scalar potentials, $\delta\mathbf{A}_{KS}$ and δv_{KS}, are linear functionals in terms of $\delta\mathbf{A}$, $\delta\mathbf{j}$ and $\delta\rho$ such that

$$
\delta\mathbf{A}_{KS}(\mathbf{r},\omega) = \frac{1}{c}(\mathbf{A}_0(\mathbf{r},\omega)+\delta\mathbf{A}(\mathbf{r},\omega)) + \int \mathbf{f}_{xc}(\mathbf{r},\mathbf{r}',\omega)\delta\mathbf{j}(\mathbf{r}',\omega)d\mathbf{r}', \tag{2.2}
$$

and

$$
\delta v_{KS}(\mathbf{r},\omega) = \int \frac{\delta\rho(\mathbf{r}',\omega)}{|\mathbf{r}-\mathbf{r}'|}d\mathbf{r}' + \int f_{xc}(\mathbf{r},\mathbf{r}',\omega)\delta\rho(\mathbf{r}',\omega)d\mathbf{r}', \tag{2.3}
$$

with $\mathbf{f}_{xc} = \delta\mathbf{A}_{xc}/\delta\mathbf{j}$ and $f_{xc} = \delta v_{xc}/\delta\rho$ being the tensor and scalar xc-kernels respectively. Note that ($\delta\mathbf{j}$, $\delta\rho$) in the above equation satisfy the the continuity equation in the frequency domain such that

$$
\delta\rho = \frac{1}{i\omega}\nabla\cdot\delta\mathbf{j}\ . \tag{2.4}
$$

The tensorial Green function $\mathbf{G}$ can be given as

$$
\mathbf{G}(\mathbf{r}-\mathbf{r}') = \frac{e^{iq|\mathbf{r}-\mathbf{r}'|}}{|\mathbf{r}-\mathbf{r}'|}\mathbf{I} + \frac{1}{q^2}\left(\frac{e^{iq|\mathbf{r}-\mathbf{r}'|}}{|\mathbf{r}-\mathbf{r}'|} - \frac{1}{|\mathbf{r}-\mathbf{r}'|}\right)\nabla'\nabla', \tag{2.5}
$$

where $q=\omega/c$ is the wavenumber in vacuum. The linear response function is given by

$$
\begin{aligned}
&\chi_{\alpha\beta}(\mathbf{r},\mathbf{r}',\omega) \\
&= \sum_{ia} f_i\left[\left(\frac{\psi_i(\mathbf{r})\alpha\psi_a(\mathbf{r})\psi_a(\mathbf{r}')\beta\psi_i(\mathbf{r}')}{\epsilon_i-\epsilon_a+\omega}\right) - \left(\frac{\psi_i(\mathbf{r})\alpha\psi_a(\mathbf{r})\psi_a(\mathbf{r}')\beta\psi_i(\mathbf{r}')}{\epsilon_a-\epsilon_i+\omega}\right)^*\right],
\end{aligned} \tag{2.6}
$$

where i and a run over the occupied and unoccupied KS orbitals, respectively. The electron density operator $\boldsymbol{\rho} = 1$ and the following paramagnetic current density operator should be substituted for α and β in (2.6):

$$
\mathbf{j}_p = -i(\nabla-\nabla^\dagger)/2, \tag{2.7}
$$

with $\nabla^\dagger$ acting on all terms to the left.

2.2. P-matrix formulation. To further simply the notations, we choose the following spectral representations for the current and electron densities:

$$\begin{cases} \delta\mathbf{j}(\mathbf{r},\omega) = \displaystyle\sum_{ia} f_i \frac{-\omega}{\epsilon_i-\epsilon_a}\psi_i(\mathbf{r})\mathbf{j}_p\psi_a(\mathbf{r})\big[P_{ai}(\omega)-P_{ia}(\omega)\big], \\ \delta\rho(\mathbf{r},\omega) = \displaystyle\sum_{ia} f_i \psi_i(\mathbf{r})\psi_a(\mathbf{r})\big[P_{ai}(\omega)-P_{ia}(\omega)\big], \end{cases} \tag{2.8}$$

with the P-matrix elements defined to be

$$\begin{aligned} &P_{ml}(\omega) \\ &=\frac{\dfrac{-\omega}{\epsilon_l-\epsilon_m}\displaystyle\int \psi_m(\mathbf{r})\mathbf{j}_p\psi_l(\mathbf{r})\cdot\delta\mathbf{A}_{KS}(\mathbf{r},\omega)d\mathbf{r}+\int\psi_m(\mathbf{r})\psi_l(\mathbf{r})\delta v_{KS}(\mathbf{r},\omega)d\mathbf{r}}{\epsilon_l-\epsilon_m+\omega}, \end{aligned} \tag{2.9}$$

for $\{m,l\}=\{i,a\}$ or $\{a,i\}$. Substituting (2.8) into the first two equations in (2.1) leads to

$$\begin{cases} \delta\mathbf{A}(\mathbf{r},\omega) = \displaystyle\sum_{ia} f_i \frac{\omega}{c(\epsilon_i-\epsilon_a)} \\ \qquad\qquad \times\displaystyle\int \mathbf{G}(\mathbf{r}-\mathbf{r}')\psi_i(\mathbf{r}')\mathbf{j}_p\psi_a(\mathbf{r}')\mathbf{r}'\big[P_{ai}(\omega)-P_{ia}(\omega)\big], \\ \delta\phi(\mathbf{r},\omega) = \displaystyle\sum_{ia} f_i\int\frac{\psi_i(\mathbf{r}')\psi_a(\mathbf{r}')}{|\mathbf{r}-\mathbf{r}'|}d\mathbf{r}'\big[P_{ai}(\omega)-P_{ia}(\omega)\big]. \end{cases} \tag{2.10}$$

By eliminating ($\mathbf{A}_{KS}$, v_{KS}) and ($\delta\mathbf{j}$, $\delta\rho$) in (2.2)-(2.3), (2.8) and (2.9), we arrive at a linear equation satisfied by the elements of the P-matrix such that for n and n' running over occupied and unoccupied orbitals, we have

$$\begin{cases} P_{nn'}(\omega) \;-\; \displaystyle\sum_{ia}\frac{K_{nn',ia}(\omega)+M_{nn',ai}(\omega)}{\epsilon_{n'}-\epsilon_n+\omega}P_{ai}(\omega) \\ \qquad\qquad +\displaystyle\sum_{ia}\frac{K_{nn',ia}(\omega)+M_{n'n,ia}(\omega)}{\epsilon_{n'}-\epsilon_n+\omega}P_{ia}(\omega) \\ \qquad = \dfrac{-q}{(\epsilon_{n'}-\epsilon_n+\omega)(\epsilon_{n'}-\epsilon_n)}\displaystyle\int\psi_n(\mathbf{r})\mathbf{j}_p\psi_{n'}(\mathbf{r})\mathbf{A}_0(\mathbf{r},\omega)d\mathbf{r}, \\ P_{n'n}(\omega) \;-\; \displaystyle\sum_{ia}\frac{K_{n'n,ai}(\omega)+M_{n'n,ia}(\omega)}{\epsilon_n-\epsilon_{n'}+\omega}P_{ai}(\omega) \\ \qquad\qquad +\displaystyle\sum_{ia}\frac{K_{n'n,ai}(\omega)+M_{nn',ai}(\omega)}{\epsilon_n-\epsilon_{n'}+\omega}P_{ia}(\omega). \\ \qquad = \dfrac{-q}{(\epsilon_n-\epsilon_{n'}+\omega)(\epsilon_n-\epsilon_{n'})}\displaystyle\int\psi_{n'}(\mathbf{r})\mathbf{j}_p\psi_n(\mathbf{r})\mathbf{A}_0(\mathbf{r},\omega)d\mathbf{r}, \end{cases} \tag{2.11}$$

where the coupling matrix $K_{nn',ia}$ is given as

$$\begin{aligned} &K_{nn',ia}(\omega) \\ &\quad=\frac{\omega^2 f_i}{(\epsilon_{n'}-\epsilon_n)(\epsilon_i-\epsilon_a)}\int\psi_n(\mathbf{r})\mathbf{j}_p\psi_{n'}(\mathbf{r})\mathbf{f}_{xc}(\mathbf{r},\mathbf{r}',\omega)\psi_i(\mathbf{r}')\mathbf{j}_p\psi_a(\mathbf{r}')d\mathbf{r}d\mathbf{r}' \\ &\quad+f_i\int\psi_n(\mathbf{r})\psi_{n'}(\mathbf{r})\left(\frac{1}{|\mathbf{r}-\mathbf{r}'|}+f_{xc}(\mathbf{r},\mathbf{r}',\omega)\right)\psi_i(\mathbf{r}')\psi_a(\mathbf{r}')d\mathbf{r}d\mathbf{r}', \end{aligned} \tag{2.12}$$

and the radiative correction $M_{nn',ia}$ has the form:

$$M_{nn',ia}(\omega) = \frac{-\omega^2 f_i}{c^2(\epsilon_n-\epsilon_{n'})(\epsilon_i-\epsilon_a)}\int \psi_n(\mathbf{r})\mathbf{j}_p\psi_{n'}(\mathbf{r})\mathbf{G}(\mathbf{r}-\mathbf{r}')\psi_i(\mathbf{r}')\mathbf{j}_p\psi_a(\mathbf{r}')d\mathbf{r}d\mathbf{r}'. \tag{2.13}$$

The above formulations (2.11) can be put in a compact form for the P-matrix elements:

$$\left[\begin{pmatrix} \mathbf{S} & \mathbf{T} \\ \mathbf{T} & \mathbf{S} \end{pmatrix} - \omega \begin{pmatrix} \mathbf{I} & \mathbf{0} \\ \mathbf{0} & \mathbf{-I} \end{pmatrix}\right] \begin{pmatrix} \mathbf{P} \\ \mathbf{P'} \end{pmatrix} = \begin{pmatrix} \mathbf{F} \\ \mathbf{-F} \end{pmatrix}, \tag{2.14}$$

with

$$\begin{aligned} &\mathbf{P}_{nn'} = P_{nn'}, \quad \mathbf{P'}_{n'n} = P_{n'n}, \\ &\mathbf{S}_{nn',ia} = \delta_{in}\delta_{an'}(\epsilon_i-\epsilon_a) - K_{nn',ia} - M_{nn',ia}, \\ &\mathbf{T}_{nn',ia} = K_{nn',ia} + M_{nn',ia}, \\ &\mathbf{F}_{nn'} = \frac{q}{\epsilon_{n'}-\epsilon_n}\int \psi_n(\mathbf{r})\mathbf{j}_p\psi_{n'}(\mathbf{r})\mathbf{A}_0(\mathbf{r},\omega)d\mathbf{r}. \end{aligned}$$

Furthermore, if we denote $\mathcal{P}_{nn'} = P_{nn'} - P_{n'n}$, then from (2.14) by addition and subtraction, we can get a linear system on $\mathcal{P}_{nn'}$ such that

$$(\mathcal{S} - \omega^2\mathbf{I})\mathcal{P} = \mathcal{F}, \tag{2.15}$$

with

$$\begin{aligned} &\mathcal{S}_{nn',ia} = \delta_{in}\delta_{an'}(\epsilon_i-\epsilon_a)^2 - 2(\epsilon_n-\epsilon_{n'})(K_{nn',ia}+M_{nn',ia}), \\ &\mathcal{F}_{nn'} = 2(\epsilon_n-\epsilon_{n'})\mathbf{F}_{nn'}. \end{aligned} \tag{2.16}$$

The radiative correction $M_{nn',ia}$ is a consequence of the coupling of Maxwell equations and the linear response theory of TD-CDFT. Without the first two equations in (2.1), there will be no $M_{nn',ia}$ in (2.14), which will be reduced to the standard linear response within TD-CDFT [**13**].

2.3. Resonance conditions. Besides the self-consistent determination of the induced EM field and current density, the linear system (2.14) (or equivalently (2.15)) also enables us to determine the resonant eigenmodes of the nano-optical structure. Resonant eigenmodes exist for particular frequencies such that the matrix in (2.14) or (2.15) is degenerate, which are called self-sustaining (SS) modes [**8**]. The resonant structure of optical spectra in general can be determined by the SS modes. Therefore, we can solve

$$\det\left(\begin{pmatrix} \mathbf{S} & \mathbf{T} \\ \mathbf{T} & \mathbf{S} \end{pmatrix} - \omega \begin{pmatrix} \mathbf{I} & \mathbf{0} \\ \mathbf{0} & \mathbf{-I} \end{pmatrix}\right) = 0, \quad \text{or} \quad \det\left(\mathcal{S} - \omega^2\mathbf{I}\right) = 0, \tag{2.17}$$

to determine the eigenfrequencies ω. In particular, we can treat it as an eigenvalue problem to determine the eigenfrequencies ω for the above matrix to have zero eigenvalues.

3. The Self-Consistent Multiscale Method

The Maxwell equations are solved on a much larger domain with a coarse grid compared with the smaller domain and a finer grid for TD-CDFT. In order to deal with the multiscale challenge, we propose a multiscale scheme which consists of two solvers: TD-CDFT serving as a **micro solver** $\mathcal{T}_l$ for the current density and the electron density and a **macro solver** $\mathcal{M}_d$ for the Maxwell equations. A self-consistent iteration is adopted to find the solution of the coupled system (2.1), which will lead to the following procedure:

(1) **Micro solver**: at each step indexed by k, with inputs $(\delta\mathbf{A}_k, \delta\phi_k)$, update the induced current and electron densities through the linear response of TD-CDFT, i.e.,
$$(\delta\mathbf{j}_{k+1}, \delta\rho_{k+1}) = \mathcal{T}_l(\delta\mathbf{A}_k, \delta\phi_k),$$
(2) **Macro solver**: with $(\delta\mathbf{j}_{k+1}, \delta\rho_{k+1})$ as fixed parameters, solve the Maxwell equations to update the EM field such that
$$(\delta\mathbf{A}_{k+1}, \delta\phi_{k+1}) = \mathcal{M}_d(\mathbf{j}_{k+1}, \rho_{k+1}),$$
(3) Repeat until a self-consistent solution is reached.

The micro-solver $\mathcal{T}_l$ can be designed to first solve the equation for the P-matrix (2.15) then obtain the current and electron densities through (2.8). The matrix-vector product $\mathcal{S}_k \cdot \mathcal{P}$ can be obtained for any vector $\mathcal{P}$ as the following:

(3.1)
$$\begin{aligned}[\mathcal{S}_k \cdot \mathcal{P}]_{nn'} =&(\epsilon_n - \epsilon_{n'})^2\mathcal{P}_{nn'} + (\epsilon_n - \epsilon_{n'}) \int \psi_{n'}(\mathbf{r})\psi_n(\mathbf{r})\delta v_{KS}(\mathbf{r})d\mathbf{r} \\ &+ 2\omega\Big(\int \psi_{n'}(\mathbf{r})\mathbf{j}_p\psi_n(\mathbf{r})\delta\mathbf{A}(\mathbf{r})d\mathbf{r} + \int \psi_{n'}(\mathbf{r})\mathbf{j}_p\psi_n(\mathbf{r})\delta\mathbf{A}_{xc}(\mathbf{r})d\mathbf{r}\Big),\end{aligned}$$

where the right hand side is determined by δA_k and $\delta\phi_k$ through (2.2)-(2.3). Due to the self-consistent structure of the above algorithm, we do not have to pursue an exact solution of (2.15). Instead, a Krylov subspace method will be used to solve (2.15) approximately. For the macro-solver, we can choose a standard scheme such as Finite Difference Method, Finite Element Method, Fast Multipole Method, etc. At each iteration, linear interpolation is used to provide the missing data due to the mismatch between the macro and micro meshes, which essentially allows communications between the macro variable of the EM field and the micro variable of the current and electron densities. The initial EM field $(\delta\mathbf{A}_0, \delta\phi_0)$ can be chosen to be the incident light.

4. Numerical Examples

We present a model calculation of resonant Scanning Near-Field Optical Microscopy (SNOM) as in Figure 1. A substrate supporting the samples is modeled by a semi-infinite local dielectric which occupies the half-space $z < 0$. For our numerical experiments, we choose both the samples and the probe as Copper(I) chloride (CuCl). The Maxwell equations are solved with a locally adaptively refined triangular mesh. The ground state occupied and unoccupied KS orbitals are computed with the OCTOPUS package [**14**]. The local density approximation (LDA) and adiabatic local density approximation (ALDA) are used for v_{xc} for ground state and

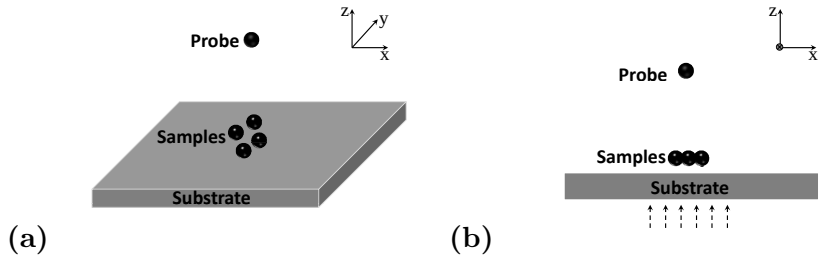

FIGURE 1. SNOM model. (a) model; and (b) example of collection mode: dashed arrows indicate the direction of incident light.

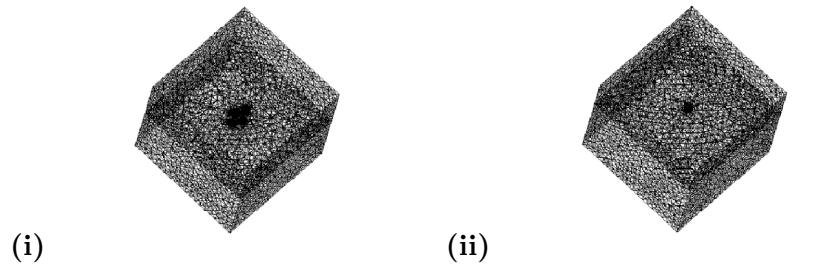

FIGURE 2. Tetrahedral meshes for solving Maxwell equations: meshes are refined near samples (i) and near probe (ii).

time dependent cases respectively [**15, 16**]. For simplicity, the vector xc-potential $\mathbf{A}_{xc}$ is ignored here.

We first compute the resonant conditions for the model corresponding to different positions of the probe, which is performed by solving the eigenvalue proble as in last section. Table 1 shows the computed lowest eigenvalues. The results show that the position of the probe have very small impact on the resonant conditions. Next we verify our computation of the lowest eigenvalues corresponding to different positions of the probe. The incident field is chosen to be

$$\mathbf{A}_0(\mathbf{r},\omega) = -ic\mathbf{p}\exp\left(i\omega/c\mathbf{d}\cdot\mathbf{r}\right)/\omega, \tag{4.1}$$

with polarization $\mathbf{p} = (p_x, p_y, p_z)$ and incident direction $\mathbf{d} = (d_x, d_y, d_z)$ such that $||\mathbf{p}|| = 1, ||\mathbf{d}|| = 1$ and $\mathbf{p}\cdot\mathbf{d} = 0$. With this incident field and given frequencies, we solve (2.15) to get the induced current density and the induced EM field. Then we compute the induced dipole moment given as

$$\delta\mu(\omega) = \frac{i}{\omega}\int \delta\mathbf{j}(\mathbf{r},\omega)d\mathbf{r}. \tag{4.2}$$

The induced dipole moment and the EM field are related through the linear polarizability $\vec{\alpha}$ as

$$\delta\mu = \vec{\alpha}\delta\mathbf{E}; \quad \vec{\alpha} = \begin{pmatrix} \alpha_{xx} & \alpha_{xy} & \alpha_{xz} \\ \alpha_{yx} & \alpha_{yy} & \alpha_{yz} \\ \alpha_{zx} & \alpha_{zy} & \alpha_{zz} \end{pmatrix}. \tag{4.3}$$

Hence we can compute $\vec{\alpha} = \frac{\delta\mu}{\delta\mathbf{E}}$. In particular, we compute $\text{aver}(\alpha) \equiv (\alpha_{xx} + \alpha_{yy} + \alpha_{zz})/3$ at the probe. Figure 3 shows the imaginary part of $\text{aver}(\alpha)$. We observe a peek at

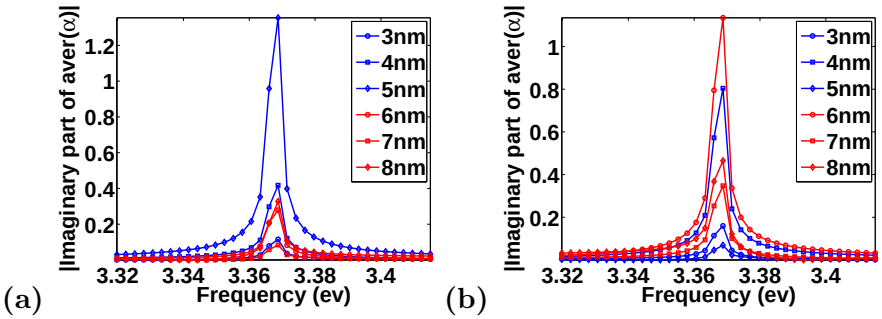

FIGURE 3. Imaginary part of aver(α) corresponding to different position of the probe: (a) $s_x = 0nm$, $s_y = 2.6nm$ and (b) $s_x = 0nm$, $s_y = 0nm$. s_z is indicated in the figure.

$\omega \approx 3.368(ev)$ which confirms that it is a resonant mode, and the result coincides with the calculation for the eigenvalue value problem (2.17).

5. Adaptive Methods for the Kohn-Sham Equation

A lot of work has been devoted to developing numerical methods for DFT and TDDFT . So far, the plane-wave expansion method (PWE) [**17**] is the most popular. Despite its successes, the PWE method still has limitations. For example, it is nontrivial to deal with the problem with non-periodic boundary condition, or to implement a parallel version because of the scaling problem. These limitations motivate the development of the real-space methods for solving the Kohn-Sham equation such as the finite difference method (FDM) [**18, 19**], the finite volume method (FVM) [**20**], finite element method (FEM)[**21**], discontinuous Galerkin method (DGM)[**22**], and mesh-free method (MFM)[**23**].

In [**3, 24**], the h-adaptive finite element method is introduced for solving the Kohn-Sham equation. Different from other adaptive methods, the mesh topology is changed after the refinement and/or coarsening. An efficient method is necessary to manage the mesh data, which is done by using a specific data structure for the mesh grid. For example, a hierarchical geometry tree (HGT) is utilized for this purpose in [**3**]. With HGT, the mesh refinement and/or coarsening can be easily organized, and an efficient interpolation mechanism between two different meshes can also be obtained. A numerical example is presented in Figure 4, in which a diborane molecule is simulated with the total energy successfully converging to the reference data (-52.628 a.u.). In [**25**], an hp-adaptive method is proposed for solving

TABLE 1. Computed lowest eigenvalues corresponding to different positions of the probe: $s_x = 0nm$, $s_y = 0nm$ or $s_y = 2.6nm$, and $s_z = (2, 3, 4, 5, 6, 7)nm$.

s_z	$3nm$	$4nm$	$5nm$	$6nm$	$7nm$
			$s_y = 2.6nm$		
$\omega(ev)$	3.36761629	3.36759775	3.36761463	3.36757544	3.36761282
			$s_y = 0nm$		
$\omega(ev)$	3.36755793	3.36761002	3.36761394	3.36760513	3.36758880

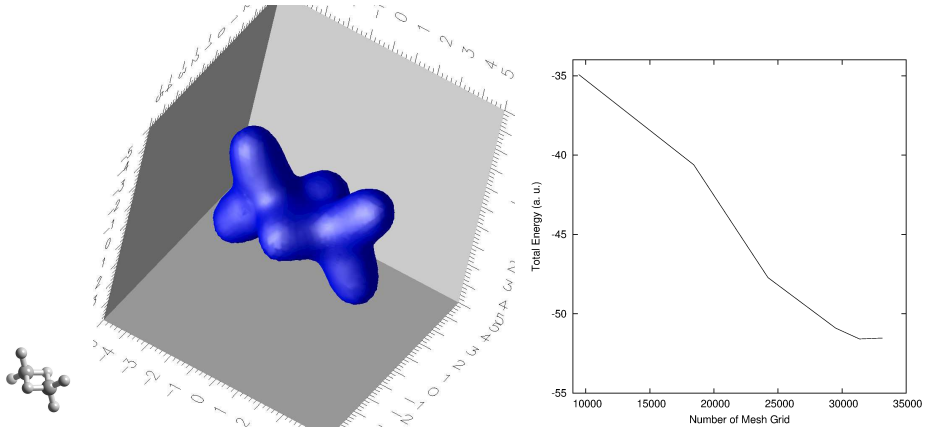

FIGURE 4. Left: The isosurface for a diborane molecule. Right: The convergence curve. In this simulation, the h-adaptive finite element method is used.

the Kohn-Sham equation, i.e., besides locally refining and/or coarsening the mesh, the order of the approximate polynomial is also locally enriched.

The r-adaptive method for the Kohn-Sham equation can be found in [**4**]. Different from the h-adaptive method which changes the mesh topology, the r-adaptive method optimizes the distribution of the grid points in the mesh, while keeping the mesh topology unchanged. The general idea is to use a geometry transformation which maps a regular mesh on a domain to a nonuniform mesh on a different domain. An early attempt of the r-adaptive method for the Kohn-Sham equation can be found in [**26**] based on the curvilinear coordinate method. The strategy proposed in [**4**] is to use a harmonic map to optimize the distribution of the mesh grids in the vicinities of the atoms. Compared with the curvilinear coordinate method, the scheme with the harmonic maps can totally separate solving PDEs from redistributing the mesh grids, which makes the code reusable for the mesh redistribution.

6. Concluding Remarks

To study the response of a system under the influence of a weak perturbation, it has been shown that the linear response theory is a quite efficient computational framework. However, this is not the situation when the perturbation of a system is significantly large. In this case, the high order terms in the response function must be taken into account, and a time propagation method should be adopted. A remarkable challenge for the time propagation method is that it is very demanding computationally. Preliminary results on adaptive methods for TDDFT [**27**] have turned out to be promising. A even greater challenge is to overcome the time scale separation between the EM field and the charged particles.

References

[1] G. Bao, D. Liu and S. Luo, *A multiscale method for optical responses of nano structures*, submitted.

[2] G. Bao, D. Liu and S. Luo, *Multi-scale modeling and computation of nano-optical responses*, submitted.

[3] G. Bao, G. Hu and D. Liu, *An h-adaptive finite element solver for the calculations of the electronic structures*, Journal of Computational Physics, 231, 4967-4979, 2012.

[4] G. Bao, G. Hu and D. Liu, *Numerical solution of the Kohn-Sham equation by finite element methods with an adaptive mesh redistribution technique*, Journal of Scientific Computing, to appear.

[5] C. Cohen-Tannoudji and J. Dupont-Roc and G. Grynberg, *Photons and Atoms: Introduction to Quantum Electrodynamics*, Wiley, New York, 1989.

[6] A. Stahl and I. Balslev, *Electrodynamics of the Semiconductor Band Edge*, Springer Tract in Mod. Phys. 110, Springer-Verlag, New York, 1987.

[7] O. Keller, *Local fields in the electrodynamics of mesoscopic media*, Phys. Rep., 268, 85-262, 1996.

[8] K. Cho, *Optical Response of Nanostructures: Microscopic Nonlocal Theory*, Springer, New York, 2003.

[9] E. Runge and E. K. U. Gross, *Density-functional theory for time-dependent systems*, Phys. Rev. Lett., 52, 997-1000, 1984.

[10] S. K. Ghosh and A. K. Dhara, *Density-functional theory of many-electron systems subjected to time-dependent electric and magnetic fields*, Phys. Rev. A, 38, 1149-1158, 1988.

[11] M. E. Casida, *Time-dependent density functional response theory for molecules*, In Recent advances in density functional methods; D. P. Chong, Ed. World Scientific, Singapore, 155-193, 1995.

[12] G. Vignale, *Current-dependent exchange-correlation potential for dynamical linear response theory*, Phys. Rev. Lett., 77, 2037-2040, 1996.

[13] M. van Faassen and P. L. de Boeij and R. van Leeuwen and J. A. Berger and J. G. Snijders, *Application of time-dependent current-density-functional theory to nonlocal exchange-correlation effects in polymers*, J. Chem. Phys., 118, 1044-1053, 2003.

[14] A. Castro and H. Appel and M. Oliveira and C. A. Rozzi and X. Andrade and F. Lorenzen, and M. A. L. Marques, *Octopus: a tool for the application of time-dependent density functional theory*, Phys. Stat. Sol. B, 243, 2465-2488, 2006.

[15] C. Fiolhais and F. Nogueira and M. A. L. Marques (Editors), *A Primer in Density Dunctional Theory*, Lect. Notes Phys. 620, Springer-Verlag, New York, 2003.

[16] M. A. L. Marques and C. A. Ullrich and F. Nogueira and A. Rubio and K. Burke and E. K. U. Gross (Editors), *Time-Dependent Density Functional Theory*, Lect. Notes Phys. 706, Springer, Heidelberg, 2006.

[17] C. Yang, J. C. Meza, B. Lee, and L. W. Wang, *KSSOLV: A Matlab toolbox for solving the Kohn-Sham equations*, ACM Trans. Math. Software, 36, 1-35, 2009.

[18] J. R. Chelikowsky, N. Troullier, and Y. Saad, *Finite-difference-pseudopotential method: Electronic structure calculations without a basis*, Phys. Rev. Lett., 72, 1240-1243, 1994.

[19] J. L. Fattebert, M. B. Nardelli, *Finite difference methods for ab initio electronic structure and quantum transport calculations of nanostructures*, Handbook of Numerical Analysis, 10, 571-612, 2003

[20] X. Y. Dai, X. G. Gong, Z. Yang, D. E. Zhang, and A. H. Zhou, *Finite volume discretizations for eigenvalue problems with applications to electronic structure calculations*, Multiscale Modeling & Simulation, 9, 208-240, 2011.

[21] J. E. Pask, and P. A. Sterne, *Finite element methods in ab initio electronic structure calculations*, Modelling Simul. Mater. Sci. Eng., 13, R71, 2005.

[22] L. Lin, J. F. Lu, L. X. Ying, and W. E, *Adaptive local basis set for KohnSham density functional theory in a discontinuous Galerkin framework I: Total energy calculation*, J. Comput. Phys., 231, 2140-2154, 2012.

[23] P. Suryanarayana, K. Bhattacharya, and M. Ortiz, *A mesh-free convex approximation scheme for KohnSham density functional theory*, J. Comput. Phys., 230, 5226-5238, 2011.

[24] D. E. Zhang, L. H. Shen, A. H. Zhou, and X. G. Gong, *Finite element method for solving KohnSham equations based on self-adaptive tetrahedral mesh*, Phys. Lett. A, 372, 5071-5076, 2008.

[25] T. Torsti, T. Eirola, J. Enkovaara, T. Hakala, P. Havu, V. Havu, T. Höynälänmaa, J. Ignatius, M. Lyly, I. Makkonen, T. T. Rantala, J. Ruokolainen, K. Ruotsalainen, E. Räs"anen,

H. Saarikoski, and M. J. Puska. *Three real-space discretization techniques in electronic structure calculations.* Physica Status Solidi (b), 243, 1016-1053, 2006.

[26] E. Tsuchida, and M. Tsukada, *Adaptive finite-element method for electronic-structure calculations*, Phys. Rev. B, 54, 7602-7605, 1996.

[27] G. Bao, G. Hu and D. Liu, *An h-adaptive finite element solver to the calculations of the electronic structures: extension to the time-dependent case*, in preparation.

Department of Mathematics, Zhejiang University, Hangzhou 310027, China, and Department of Mathematics, Michigan State University, East Lansing, MI 48824.
E-mail address: bao@math.msu.edu

Department of Mathematics, University of Macau, Macau, China.
E-mail address: garyhu@umac.mo

Department of Mathematics, Michigan State University, East Lansing, MI 48824.
E-mail address: richardl@math.msu.edu

Department of Mathematics, Iowa State University, Ames, IA 50011.
E-mail address: luos@iastate.edu